Measurement 259 (2026) 119623

Contents lists available at ScienceDirect

Measurement

journal homepage: www.elsevier.com/locate/measurement

Advancing metrological performance of a calorimetric absorbed dose-to-water primary standard for medium energy X-ray beams☆

Susy Toma [a,b,*], Massimo Pinto [b], Fausto Arpino [c], Domenico Capriglione [a]

[a] Dept. of Electrical and Information Engineering, University of Cassino and Southern Lazio, Italy
[b] National Institute of Ionizing Radiation Metrology ENEA-INMRI, Rome, Italy
[c] Dept. of Civil and Mechanical Engineering, University of Cassino and Southern Lazio, Italy

ARTICLE INFO

Keywords:
Graphite calorimetry
Calorimetry
Medium-energy x-rays
Reference dosimetry
Primary standard
X-ray dosimetry
Measurement uncertainty

ABSTRACT

This study presents an advancement in the metrological performance of the graphite calorimeter in a water phantom developed at ENEA-INMRI, which serves as the Italian primary standard for absorbed dose to water in medium-energy X-ray beams. Through the optimization of key electrical parameters, a significant reduction in the Type A uncertainty associated with the fractional resistance change of the main thermistor was achieved. This improvement enhances measurement stability and repeatability, contributing to the overall refinement of the standard's uncertainty budget. Given the limited number of absorbed dose to water standards available worldwide in this energy range, the enhancement of the Italian standard reinforces its relevance within the international metrology community and supports future interlaboratory comparisons and harmonization efforts.

1. Introduction

Over the past two decades, Primary Standard Dosimetry Laboratories (PSDLs) have significantly advanced their primary standards based on state-of-the-art technology, scientific expertise, and rigorous metrological principles; these standards are designed to ensure high levels of traceability and accuracy, typically employing calorimetric methods in the determination of absorbed dose to water. IAEA TRS-398 Code of Practice plays a crucial role in clinical dosimetry by providing standardized procedures for the calibration of ionization chambers. These procedures assume the existence of robust, well-characterized standards from PSDLs, enabling their effective dissemination to radiotherapy departments through traceable calibration services [1].

The accurate determination of the quantity absorbed dose to water D_w is a cornerstone of radiotherapy, as it is the measurement basis for treatment efficacy and patient safety. Absorbed dose to water, D_w, is defined as the amount of energy imparted by ionizing radiation to a unit mass of water. It is expressed in grays (Gy), where 1 Gy corresponds to 1 J of energy deposited per kilogram of water. D_w serves as the reference quantity in external beam radiotherapy dosimetry, as water closely approximates the radiological properties of human tissue [2].

Three primary measurement methods are sufficiently accurate to serve as standards for the determination of absorbed dose to water: calorimetry, chemical dosimetry, and ionization dosimetry. Established procedures include water and graphite calorimetry, chemical dosimetry, and ionometry. Among these, calorimetry is considered the most fundamental, as it enables direct measurement of absorbed dose by quantifying the temperature rise in a medium subjected to ionizing radiation [3].

Low and medium-energy x-ray beams, with tube potentials ranging from 50 kV to 300 kV and an artificial separation around 70–100 kV (∼4 mm Al half-value layer, HVL), present considerable challenges for accurate dosimetry, unlike high-energy photon beams such as those from 60ˆCo sources, medium-energy x-rays historically lacked robust primary standards of absorbed dose to water, leading to greater reliance on indirect methods (based on another dosimetric quantity named air kerma) and empirical correction factors, additionally dosimetric protocols in this energy range often exhibited higher uncertainties due to the use of air kerma-based conversions, underscoring the need for direct D_w realizations to improve measurement accuracy and traceability [4]. Medium-energy x-rays are widely employed in clinical settings, particularly for the treatment of superficial non-melanoma cancers, where

☆ This article is part of a special issue entitled: 'MEASUR_XXIV IMEKO World Congress' published in Measurement.

* Corresponding author at: Dept. of Electrical and Information Engineering, University of Cassino and Southern Lazio, Italy.
E-mail addresses: susy.toma@unicas.it, susy.toma@enea.it (S. Toma), massimo.pinto@enea.it (M. Pinto), fausto.arpino@unicas.it (F. Arpino), domenico.capriglione@unicas.it (D. Capriglione).

https://doi.org/10.1016/j.measurement.2025.119623
Received 25 June 2025; Received in revised form 3 November 2025; Accepted 4 November 2025
Available online 6 November 2025

precise dose delivery is essential to ensure therapeutic efficacy and minimize damage to surrounding healthy tissue [5].

Globally, four primary standards of absorbed dose to water (D_w) in the medium-energy x-ray range have been established at national metrology institutes, with a fifth at the BIPM. These standards were compared in the international comparison EURAMET.RI(I)-S13 and more recently linked to the key comparison BIPM.RI(I)-K9 [6,7]. Most existing standards are based on water calorimetry, while the Italian standard uses graphite calorimetry in a water phantom. Comparative studies between these techniques are essential to validate their respective accuracies and to identify potential systematic deviations [8,9,10].

The Italian standard measures the temperature rise induced by ionizing radiation in its graphite core through the resistance variation of a negative temperature coefficient (NTC) thermistor [11,12].

The most recent international comparison *EURAMET.RI(I)-S13* reported the uncertainty components summarized in Table 1. Among these, two parameters were identified as primary contributors to the overall Type A uncertainty in calorimetric dose measurements. The first, f_C, denotes the fractional change in the resistance of the main thermistor and was found to be the dominant contributor, with a relative uncertainty of 0.015. The second, K_{qa}, represents the quasi-adiabatic calibration coefficient, which initially exhibited a Type A uncertainty of 0.16 %, subsequently refined to 0.11 % [13].

The present work aims to reduce the uncertainty associated with the fractional change in thermistor resistance f_C during electrical calibration and irradiation measurements, improving the repeatability of calorimetric measurements. The aim of this work is not to fully characterize the performance of a national standard that has been established before. Rather, this work considers the largest component of the uncertainty budget, which is related to repeatability, and addresses strategies to improve this specific uncertainty component.

Historically, dosimetry in the medium-energy X-ray range has relied on air kerma–based standards, which require multiple conversion steps, such as cavity theory and energy-dependent correction factors, to derive absorbed dose to water. These indirect methods introduce additional uncertainties and reduce clinical relevance, especially in complex beam conditions.

A direct calorimetric standard, by contrast, measures the energy deposited in water without intermediate conversions, aligning precisely with the quantity of interest in radiotherapy. This approach improves measurement accuracy and strengthens the calibration chain.

Absorbed dose to water is clinically meaningful, as it reflects the actual energy delivered to tissue. Establishing a robust calorimetric standard in this energy range supports the transition from legacy air kerma–based systems and ensures consistency with modern protocols such as IAEA TRS-398. Validated through international comparisons, such standards are essential for improving traceability and clinical utility in medium-energy X-ray dosimetry.

Table 1
Rx Calorimeter total uncertainty budget showed in the EURAMET.RI(I)-S13 supplementary comparison.

Source of uncertainty	u_{iA}	u_{iB}
f_C, fractional change of the thermistor resistance	0.015	0.0014
K_{qa}, quasi-adiabatic calibration coefficient	0.0016	0.0021
K_{vol}, core finite volume correction factor	0.0014	0.0010
K_{sc}, non-water equivalence of PMMA phantom's entrance window correction factor	0.0010	
Monitor chamber signal	0.0005	0.0021
Calorimeter positioning		0.0025
C_{wg}, graphite to water absorbed dose conversion factor	0.0010	0.0087
K_{mass}, graphite mass correction factor	0.0010	0.0046
Quadratic sum	0.0153	0.0107
Combined relative standard uncertainty, D_w	0.019	

The observed variability in the change of the main thermistor resistance arises from short-term fluctuations and noise in the measurement system, which we address through a different and optimized configuration of signal acquisition. Following an initial experimental campaign conducted to assess the impact of electrical parameterization on measurement stability, the calorimetric system was evaluated using a revised measurement configuration, both during the calibration phase and under irradiation conditions.

2. Materials and methods

2.1. Rx calorimeter

The ENEA-INMRI graphite calorimeter features a thermally isolated "core", separated from two surrounding structures the "Jacket" and the "Shield" by evacuated vacuum gaps. This nested configuration allows precise monitoring of temperature variations induced by radiation exposure. The realization of the graphite calorimeter was described in previous reports [14]. The theory and operation of a graphite calorimeter are designed around the concept of quickly bringing its three nested graphite bodies arranged concentrically, the "Shield," the "Jacket," and the "Core" to a state of thermal equilibrium and maintaining it long enough for an accurate measurement during exposure to a source of heat [15]. Our graphite calorimeter is "Domen type"; the graphite nested structure calorimeter was developed at NBS [16]. The disc-shaped core, which is the innermost graphite body, measures 21 mm in diameter and 2 mm in thickness and weighs 1.134 g.

ENEA-INMRI Rx calorimeter operates in a quasi-adiabatic mode, wherein core temperature rises are measured during irradiation or current injection. Quasi-adiabatic conditions are achieved by minimizing thermal exchange between the calorimeter components, thereby isolating the heat generated within the core. A vacuum level of at least 10^{-5} mbar must be maintained in order to assure that thermal interaction between the three bodies is restricted to residual radiative effects exclusively. Temperature differences are measured using NTC micro thermistors, which are positioned within each of the three graphite bodies of the calorimeter [17,18].

Components of the calorimeter can be seen in Fig. 1, the external PMMA chassis and the three graphite nested bodies, while Fig. 2 shows the calorimeter inserted into the PMMA phantom.

2.2. Measurement chain

The calorimetric system comprises three graphite bodies, each instrumented with embedded thermistors serving both heating and sensing functions. Two independent Wheatstone bridge circuits are utilized: the first monitors voltage variations across the core thermistor embedded in the central graphite body, which functions as the primary sensing element. The second bridge is configured to sequentially address the auxiliary thermistors distributed throughout the graphite assembly via a Keithley 7001 switching unit. This configuration enables comprehensive thermal monitoring while preserving high measurement fidelity. The electronic system associated with the previously described Rx calorimeter [19] incorporates three Keithley 2400 voltage/current source meters. These instruments deliver electrical power simultaneously and proportionally to the Core, Jacket, and Shield via the respective heating thermistors, with power levels scaled according to the mass of each graphite body. The complete electronic setup is illustrated in Fig. 3.

2.3. Electrical parameters

The investigation described in the following paragraph focused on three settings of nanovoltmeter Keithley 2182a connected to the calorimeter's core to assess the impact on measurement stability and resolution in the nanovolt regime: the Number of Power Line Cycles (*Nplc*),

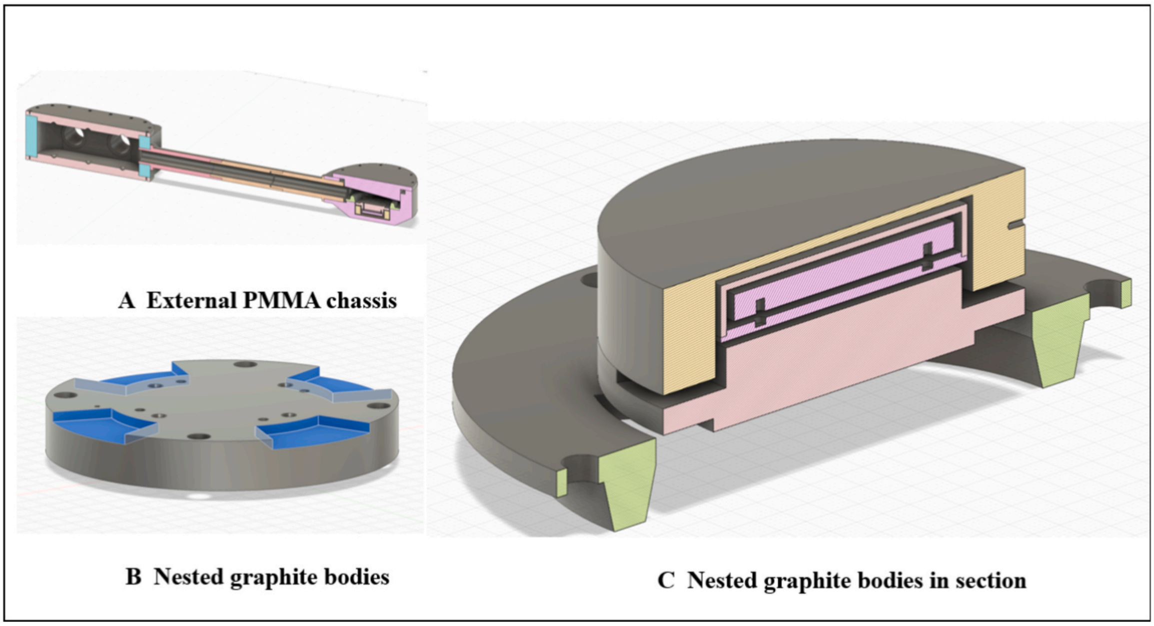

Fig. 1. The Rx calorimeter nested structure.

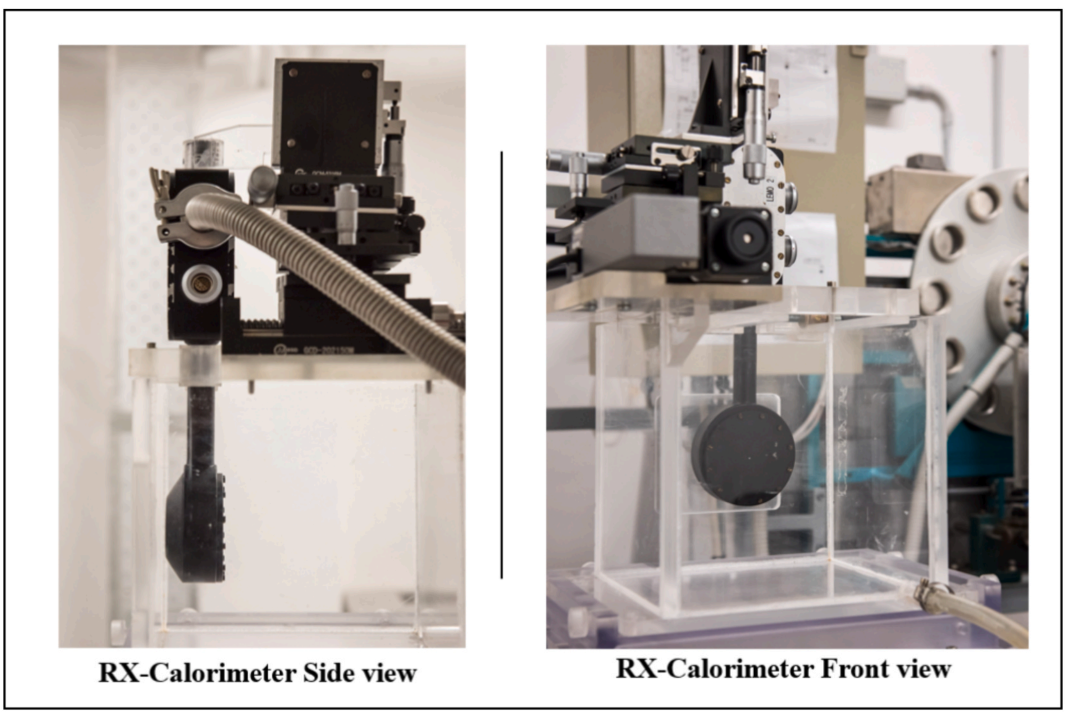

Fig. 2. Rx calorimeter in the PMMA-water phantom.

the averaging algorithm type of the built-in digital filter, and the stack size, the number of samples used for computing the filtered output, in Delta Mode operation.

Nplc: its functionality is to define the integration time for each A/D conversion, expressed in units of power line cycles. As an impact on the measurement, increasing Nplc improves noise rejection, particularly for line-frequency interference, by extending the integration time. For nanovolt-level signals, higher Nplc values (e.g., ≥5) are recommended to suppress ambient electrical noise and enhance precision [20,21]. However, this comes at the cost of slower measurement rates. In this study, the selected values for the Number of Power Line Cycles (Nplc) are moderate, with a maximum setting of 20. This configuration does not result in a significant increase in total acquisition time, nor does it compromise the temporal resolution of the measured signal. Indeed, the data acquisition time configured within the C++ software controlling the calorimeter is set to 500 ms. The ranges analyzed for both parameters, “Count” and “Nplc”, are within the data sampling time, ensuring sufficient noise rejection while maintaining the responsiveness required for high-resolution voltage measurements.

Averaging Type: it assesses the averaging algorithm applied to the measurement data by Keithley 2182a; during repeating type average mode, unlike dynamic averaging techniques, the sample group remains

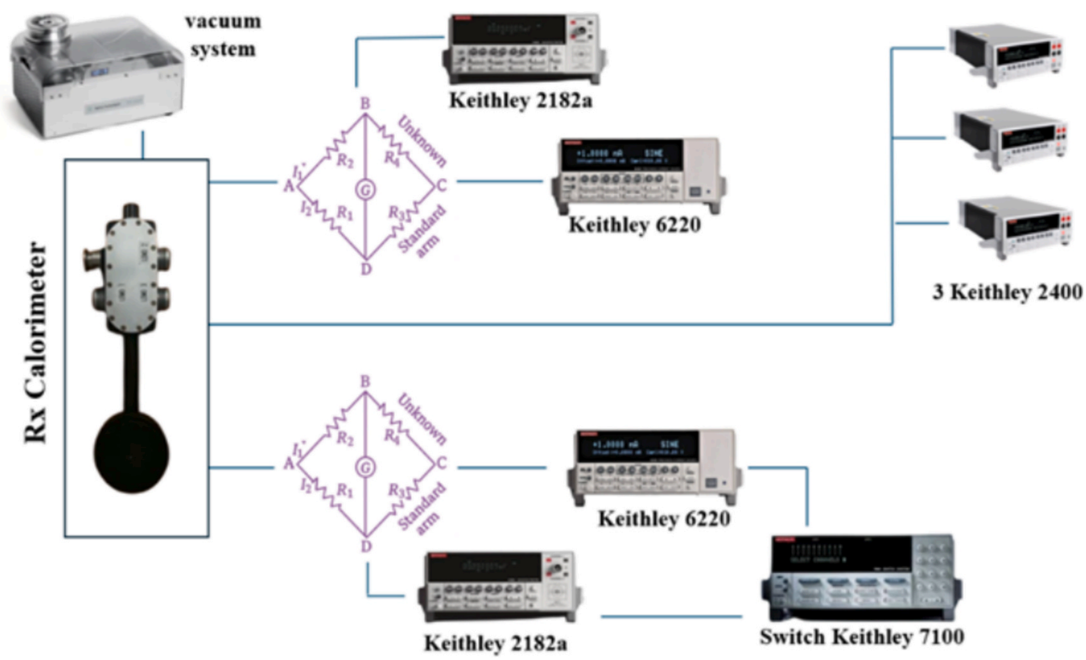

Fig. 3. Complete measurement chain of the Rx calorimeter.

unchanged during acquisition. In this mode, upon completion of the predefined number of readings, the arithmetic mean is computed and returned as a single representative value. This approach is particularly suited for quasi-static signals where temporal variation is negligible during the averaging interval [22]. In INMRI calorimetric system, the instrumental noise does not exhibit low-frequency components, and no thermal drift or slow instabilities are observed during acquisition. Under these conditions, the repeating average mode does not introduce autocorrelation among the acquired data, thereby preserving the statistical integrity of the sample set. When the measured signal is quasi-static and the noise is purely stochastic, the resulting samples can be considered statistically independent. In this study, the repeating type average mode was selected for evaluation. Count: it defines the number of consecutive measurements used in the averaging stack. Higher Count values improve statistical stability by suppressing random fluctuations, which is particularly advantageous when measuring low-level signals affected by thermal and environmental noise [22]. However, excessive averaging may compromise temporal resolution by masking transient phenomena. In this study, a moderate Count value of 20 was adopted across all configurations to ensure adequate noise suppression while preserving the signal's temporal fidelity. The configuration and the technique can also be extended to other DMMs like HP3458A, which offers very similar kinds of settings for such parameters.

Delta Mode operation: all voltage measurements on the sensing thermistor of the calorimeter core have been processed by the nanovoltmeter Keithley 2182a. A constant current of 15 μA, defined as "probe current" is injected to drive the Wheatstone bridge of the Core from the precision current source Keithley 6220. In our setup, the probe current is split equally across the bridge arms, resulting in a current of 7.5 μA through the thermistor. With a nominal resistance of 10 kΩ, the corresponding power dissipation is approximately 0.5625 μW. This low power level minimizes self-heating effects, which are further mitigated by the thermal design of the core.

The Keithley 2182A Nanovoltmeter features a Delta Mode designed to facilitate low-noise differential voltage measurements in conjunction with the 6220. In this mode, the current source alternates the polarity of the probe current, and the 2182a synchronously acquires voltage readings at each polarity [23]. By computing the difference between successive measurements, the instrument effectively cancels thermoelectric offsets and low-frequency noise, thereby enhancing measurement accuracy and stability. Delta Mode is particularly advantageous for characterizing low-resistance materials and devices, where minimizing thermal EMFs and environmental interference is critical [24]. The Wheatstone bridge of the calorimeter Core was upgraded to "Delta mode" to account for thermal noise that could have arisen from the many metal junctions that constitute the wiring from the thermistor to the measuring apparatus, that is, Pt-Ir wires, copper wires of varying thickness, and soldering tin [11]. When applying Keithley's Delta Mode to a Wheatstone bridge, constant current excitation is mandatory [23].

The Keithley Delta Mode operation is specifically designed for ultra-low-level measurements, where constant current level excitation minimizes noise and enhances sensitivity. Constant current level excitation of the Wheatstone bridge allows the operator to adjust the probe current, providing a practical means to mitigate self-heating effects in resistive sensors. Self-heating is a well-known issue in DC-excited bridges, particularly when using strain gauges or thermistors, where the power dissipated across the sensing element can distort the measurement. Adjustable current excitation provides a direct approach to minimize thermal drift and maintain measurement integrity [25]. The parameters under investigation Nplc, averaging type and Count are configurable in high-precision nanovoltmeters and digital multimeters, which are specifically designed to support ultra-low-level measurements through fine control of acquisition settings, while the delta mode functionality is fully integrated within the Keithley system, similar measurement techniques, based on current reversal and differential averaging, can be manually configured on other precision instruments through external synchronization and custom control routines.

2.4. Analytical model

Calorimetry provides a direct and absolute method for determining the absorbed dose to water D_w in medium-energy x-ray beams. The graphite calorimeter developed at ENEA-INMRI operates by measuring the temperature rise in a thermally isolated graphite body exposed to ionizing radiation. The quantity absorbed dose to water at the depth of 2 g cm^{-2} and at a source-to-surface distance (SSD) of 98.0 cm was determined in accordance with the theoretical model presented below. The absorbed dose to water D_w is defined in Eq. (1), where $d\varepsilon$ denotes the average energy transferred by ionizing radiation to a differential mass element dm of the medium:

$$D_w = \frac{d\bar{\varepsilon}}{dm} \tag{1}$$

The dose is the quotient of absorbed energy per unit mass, D_w. Our calorimeter realizes a measurement of absorbed dose to graphite, first, which is converted to absorbed dose to water in a second stage via Monte Carlo simulations of radiation transport and absorption. The absorbed dose to graphite D_g is calculated from the temperature variation according to equation (2), where c_g is the specific heat capacity of graphite and ΔT is the measured temperature rise:

$$D_g = c_g \cdot \Delta T \tag{2}$$

To estimate the average absorbed dose to water in the same volume occupied by the calorimeter core, a material conversion factor C_{wg} is applied, based on Monte Carlo simulations, which model the energy deposition characteristics of both media. The conversion factor C_{wg} is applied to translate the measured dose in graphite into the corresponding average absorbed dose in water, ensuring consistency with clinical dosimetry standards. This factor accounts for the differences in energy absorption between graphite and water and is dependent on the photon energy spectrum.

$$D_w = D_g \cdot C_{wg} \tag{3}$$

The absorbed dose at the reference point in water is determined as:

$$D_w = D_w \cdot k_{vol} \cdot k_{sc} \tag{4}$$

with K_{vol} is a factor correcting for the radial non-uniformity of the beam in the calorimeter core, and K_{sc} corrects for the non-water equivalence of the 4 mm of PMMA phantom entrance window. The effective mass of the calorimeter core during irradiation is m_c [11]. To account for the presence of foreign materials in and around the graphite core of the calorimeter, including glass and Platinum-Iridium wires, a correction is introduced to the core mass, K_{mass}, so that:

$$m_c = m_g \cdot k_{mass} \tag{5}$$

where m_g is the mass of the graphite core and K_{mass} the correction for foreign materials, which is photon energy-dependent and therefore radiation-quality dependent. The calorimeter is calibrated electrically by applying a known electrical power and measuring the corresponding temperature rise. The electrical energy E delivered during calibration is given by an integration of the injected electrical power over the run time as:

$$\mathrm{E} = \int \mathrm{V(t)\ I(t)\ dt} \tag{6}$$

by measuring the voltage V(t) across the heating thermistors and the current I(t) injected in the heating thermistors for a stated time interval t. Voltage signal is related to the measurement of the resistance variation of the thermistor of the core with a negative temperature response coefficient (NTC), defined as ΔR; $k_{hl,C}$ is a correction factor accounting for the core heat loss during irradiation, two correction factors were calculated separately, one for the energy imparted to the entire calorimeter during irradiation, and another for the point-like energy input during electrical calibration. To distinguish these cases, subscripts 'I' (irradiation) and 'C' (calibration) are used accordingly.

$f_C = \Delta R/R$ is the fractional change of core sensing thermistor resistance, recorded at each run, following the energy injection E, it is related to the energy amount received by the medium. The quasi-adiabatic calibration coefficient K_{qa} links electrical energy to the relative change in thermistor resistance, it is defined as the ratio between the electrical energy E delivered during calibration and the relative change in thermistor resistance ΔR/R. This expression reveals an inverse proportionality between K_{qa} and the measured resistance variation f_C. The inverse dependence of K_{qa} on ΔR/R reflects the sensitivity of the thermistor to thermal input. A more responsive sensor requires a smaller calibration coefficient to match the same energy input, thereby influencing the final dose calculation. This relationship is critical for interpreting the thermistor response and for ensuring accurate dose estimation.

$$k_{qa} = \frac{\frac{E}{k_{hl,C}}}{\frac{\Delta R}{R}} \tag{7}$$

This coefficient is used to interpret the resistance change observed during irradiation in terms of absorbed dose. The average absorbed dose to graphite D_g in the calorimeter core volume is realized according to the final equation:

$$\overline{D}_g = \frac{f_c \cdot k_{qa}}{m_c} \tag{8}$$

2.5. *Calorimetric run*

Each calorimetric run comprises three distinct phases: an initial drift period without input power, a heating interval during power application, and a final drift phase following power shutdown. Fig. 4 [11], illustrates the amplitude of the resistance variation (ΔR) throughout a typical calorimetric cycle. The resistance values of the thermistors prior to and following irradiation are modeled using linear regression and extrapolated to determine the variation induced by thermal input, either from ionizing radiation or electrical current injection during calibration.

The fractional change in core thermistor resistance, denoted as f_C, is evaluated by performing paired forward and backward extrapolations to the temporal midpoint of the heating interval. These extrapolations are based on linear regressions applied to resistance data acquired immediately before and after the heating phase, respectively. Each regression is computed over a 120-second acquisition window to ensure statistical robustness and minimize transient effects.

To ensure the reliability of the estimated fractional resistance change (ΔR/R), a set of criteria is applied, reflecting the characteristics of an optimal 120-second quasi-adiabatic run. First, the direction of heat flow, if non-negligible, must remain consistent before and after the heating interval. Second, the linear regressions must accurately capture the drift behavior across the entire 120-second fitting window. Third, the slope of each regression line must not exceed 0.01 $\Omega \cdot \mathrm{min}^{-1}$, corresponding to a temperature drift of less than 25 $\mu\mathrm{K} \cdot \mathrm{min}^{-1}$, thereby preserving the thermal stability required for precise extrapolation [27]. The time needed for a typical calorimetric RUN, which is about 500 s.

The first and the last points of the heating interval during power application are acquired through C++ software, they are not derived from data manipulation. The change in resistance f_C (ΔR/R) was determined using linear regression centered around the midpoint of the irradiation run, where the thermal response of the graphite calorimeter is most stable. This approach minimizes transient effects and aligns with established methodologies in calorimetric dosimetry [26].

3. Experimental results

The measurements with the Rx calorimeter took place at the National Institute of Ionizing Radiation Metrology ENEA- INMRI in the ENEA Casaccia Research Centre and at Industrial Measurements Laboratory, LAMI, of the Department of Electrical and Information Engineering DIEI of the University of Cassino and Southern Lazio.

The initial phase of the study focuses on the voltage signal measured along the diagonal of the Wheatstone bridge of the Core of the calorimeter. In this preliminary experimental configuration, only the Keithley instruments interfaced with the core Wheatstone bridge are independently connected via an auxiliary GPIB network. The analysis

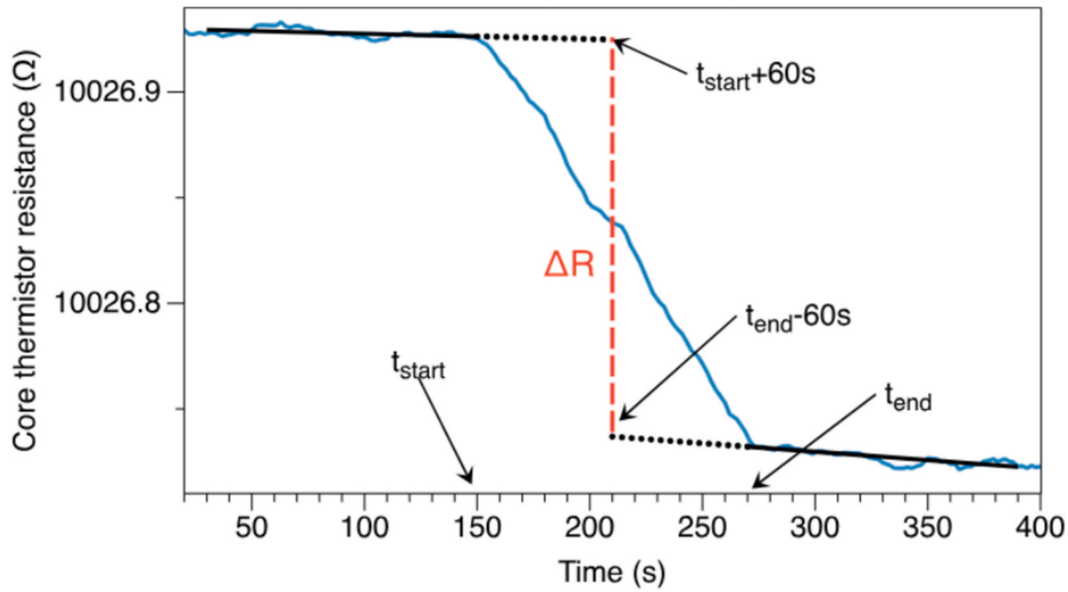

Fig. 4. Fitting procedure to estimate fractional resistance change $f_C = \Delta R/R$ used in ENEA-INMRI, (Figure with permission of the author M.Pinto).

investigates the behavior of the voltage signal and the associated electrical noise under varying acquisition parameters. The experimental setup and connection scheme are illustrated in Fig. 5.

In all configurations explored, the Keithley 2182A nanovoltmeter and the Keithley 6220 current source, both connected to the core via the auxiliary GPIB interface, were operated in delta mode, applying a constant current level of 15 μA with polarity reversal every 100 ms.

The second phase of the analysis involved repeated calorimetric runs under electrical calibration conditions. The study employed a current of 15μA to identify optimal measurement configurations aimed at minimizing Type A uncertainty in calorimetric determinations. A total of 30 calibration runs were performed, each with a heating interval of 120 s, in each different parameters configuration.

Upon injection of the calibration current via the Keithley 6220 source, connected to the Wheatstone bridge of the calorimeter core, voltage variations on the order of 1 nV were observed within approximately 2–3 s. For each set of 30 measurements, the corresponding mean value, μ30, and sample standard deviation, σ_{30}, were computed as defined in (9) and (10). Additionally, the standard deviation of the mean was evaluated according to Eq. (11).

$$\mu_{30} = \sum_{i=1}^{30} \frac{x_i}{30} \tag{9}$$

$$\sigma_{30} = \sqrt{\frac{\sum (X - \mu_{30})^2}{29}} \tag{10}$$

$$\overline{\sigma}_{30} = \frac{\sigma_{30}}{\sqrt{30}} \tag{11}$$

The influence of setting parameters on Type A uncertainty in the new electronic configuration of the Rx calorimeter was assessed by evaluating the standard deviation and the standard deviation of the mean

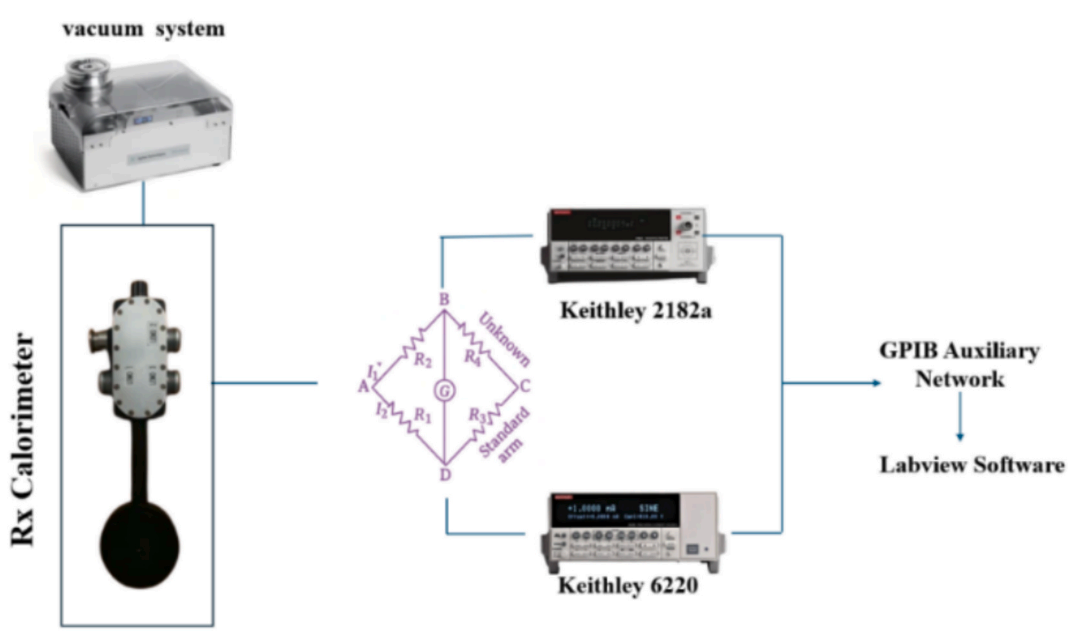

Fig. 5. Preliminary test setup scheme.

across the repeated calibration runs in two different experimental campaigns in calibration phase and in one experimental campaign under irradiation. The first measurement campaign was conducted using a calibration current of 15 μA and performing 30 calorimetric runs. Throughout these runs, the Nplc parameter was held constant at 5, while the Count parameter was varied from 5 to 40. The results are presented in the following Table 2.

The difference between the minimum and maximum mean values obtained across the four tested configurations for fixed Nplc equal to 5 is 0.08×10^{-5}, corresponding to a relative deviation of 3.44 %. This spread across the tested configurations suggests that the system maintains consistent output under the applied conditions, and that the influence of the selected parameters on the mean values of f_C in electrical calibration runs is minimal within the observed range.

The standard deviation values obtained for the four samples of runs indicate good repeatability and low variability across measurements, suggesting that the system exhibits stable behavior under the tested conditions. The lowest standard deviation and the lowest standard deviation of the mean were observed with a sample count of 20, using the tested configuration that included Delta Mode, repeated averaging, and an Nplc setting of 5.

A subsequent measurement campaign was conducted using a calibration current of 15 μA and performing 30 calorimetric runs. Throughout these runs, the Count parameter was held constant at 20, while the Nplc parameter was varied from 5 to 40. The results obtained are summarized in Table 3.

While the difference between the maximum and minimum mean values across the tested configurations is limited, equal to 0.07×10^{-5}, corresponding to a relative deviation of approximately 2.70 %, the comparison of the standard deviations of f_C across configurations with varying Nplc settings reveals significant variability. This suggests that certain parameter combinations yield more stable measurements than others. In particular, both the standard deviation and the standard deviation of the mean reach their lowest values when Nplc is set to 20, indicating improved repeatability under this configuration.

Fig. 6 presents two representative calorimetric runs performed under electrical calibration conditions, both employing a current of 15 μA and a fixed Count value of 20, but with different Nplc settings. Each run comprises approximately 500 resistance measurements and exhibits distinct levels of data dispersion, as quantified by the corresponding Root Mean Square Error (RMSE) values.

As the third and final part of this study, a comprehensive experimental setup is required to perform calorimetric runs under irradiation, ensuring accurate thermal measurements and controlled exposure conditions. This experimental setup includes an X-ray tube, a monitor chamber and a chiller system used to regulate the temperature of the water within the PMMA phantom. The calorimeter is designed to operate with horizontally directed radiation beams and is housed within a cube-shaped phantom composed of 1-cm-thick PMMA plates, with an edge length of 200 mm. The phantom is filled with thermalized water maintained at 20 °C and remains connected to the chiller system throughout the duration of the experiment to ensure thermal stability. The front window of the PMMA phantom housing the Rx calorimeter was positioned at a source-to-surface distance (SSD) of 98 cm. The irradiation source is the ENEA-INMRI medium-energy X-ray tube, a bipolar ISO-VOLT system manufactured by GE and equipped with two GE 225 kV high-voltage generators. A monitor chamber is installed in close proximity to the tube to ensure beam stability and dose monitoring. The X-ray beam is collimated to define the irradiation field and minimize scatter. The components of the experimental irradiation setup are illustrated in Fig. 7.

Table 2
Fractional change in Resistance of the calorimeter's core thermistor from the mean value during the electrical calibration runs, analysis for different Count values.

Nplc 5	f_CΔR/R (mΩ/Ω)	Mean value	Standard deviation	Standard deviation of the mean
	Count 5	2.61E−05	9.79e−07	1.79E−07
	Count 10	2.56E−05	8.71E−07	1.59E−07
	Count 20	2.53E−05	7.32E−07	1.50E−07
	Count 40	2.58E−05	8.65e−07	1.58E−07

Table 3
Fractional change in Resistance of the calorimeter's core thermistor from the mean value during the electrical calibration runs, analysis for different Nplc values.

Count 20	f_CΔR/R (mΩ/Ω)	Mean value	Standard Deviation	Standard deviation of the mean
	Nplc 5	2.52E−05	8.64e−07	1.58E−07
	Nplc 10	2.54E−05	1.1E−06	2.03E−07
	Nplc 20	2.52E−05	6.60E−07	1.21E−07
	Nplc 40	2.59E−05	9.27e−07	1.69E−07

The CCRI-250 X-ray quality was employed for the calorimetric runs conducted in this measurement campaign. A comparative analysis was performed on two sets of 40 calorimetric runs carried out in the water phantom and under irradiation at the CCRI250 X-ray quality. One dataset was acquired with the Nplc parameter set to 1 before the experiment, while the second has been acquired with the new electrical configuration and optimized settings, including Nplc set to 20. The fractional resistance change parameter during irradiation, f_C exhibited a notable reduction in both its standard deviation and its relative standard deviation of the mean, approximately 26 % in each case, the results are summarized in Table 4.

The calorimetric runs presented in Fig. 8 were performed under irradiation conditions corresponding to the CCRI-250 X-ray quality during a dedicated experimental session. In both cases, the X-ray beam delivered comparable energy to the calorimeter core, with measured values in the microjoule (μJ) range. Despite the similar energy deposition, the resistance data exhibited a marked difference in dispersion relative to the respective interpolation lines, indicating variability in measurement stability or noise characteristics.

The estimated type A uncertainty on the fractional change in thermistor resistance during irradiation is calculated as the standard deviation value of f_C normalized to the quantity Q_{mon}, corresponding to the charge signal from the monitor chamber integrated within the INMRI setup, as reported in equation (12).

$$f_c \frac{\Delta R/R}{Q_{mon}} \tag{12}$$

Table 5 shows the final results, the reduction in Type A uncertainty associated with the repeatability of $f_{C,}$ calculated as the standard deviation of the sample under irradiation observed for the X-ray quality CCRI250. Specifically, the uncertainty associated with f_C decreased from 0.015 to 0.009. Considering the updated Type A uncertainty of the quasi-adiabatic calibration factor K_{qa}, evaluated at 0.0011, the overall uncertainty budget was reduced from 0.019 to 0.014, representing a 25.3 % improvement in measurement precision.

4. Conclusions

This study has presented an improvement in the Type A uncertainty associated with the fractional resistance change of the calorimeter's main thermistor, denoted as$f_C = \Delta R/R$. This parameter is essential for the accurate determination of the absorbed dose to water (D_w) through the direct measurement of the absorbed dose to graphite (D_g). The experimental campaign enabled the identification of measurement configurations that led to a reduction of approximately 26 % in the uncertainty component related to f_C. This result reflects the enhanced stability of the calorimeter under irradiation by the X-ray beam. This

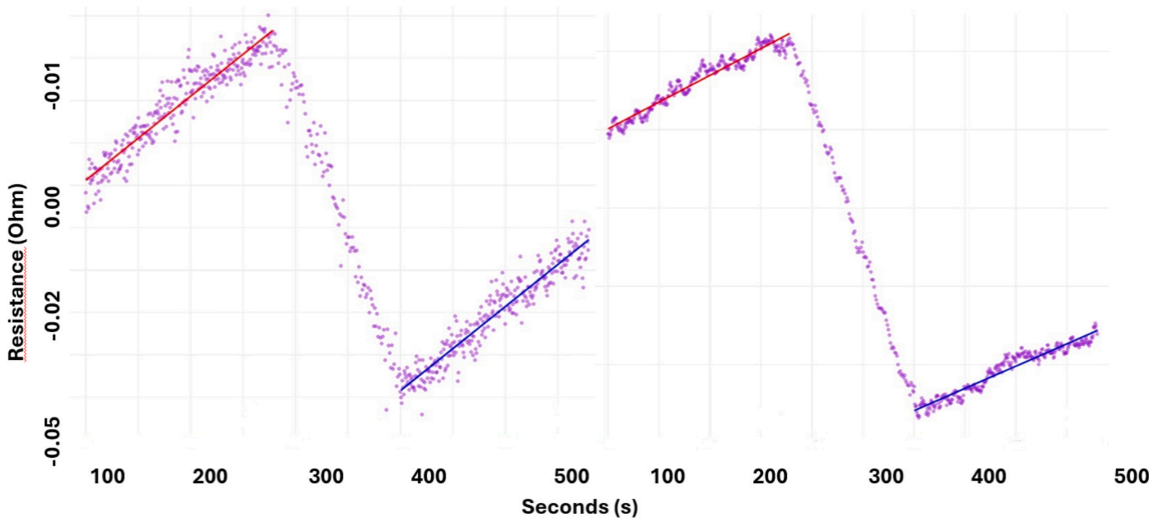

Fig. 6. Graphic calorimetric run comparison in electrical calibration (I = 15μA). On the left side a run acquired with Delta mode off, Nplc 5 and Count 5, on the right side the run acquired with Delta mode on, Nplc 5, Count 20.

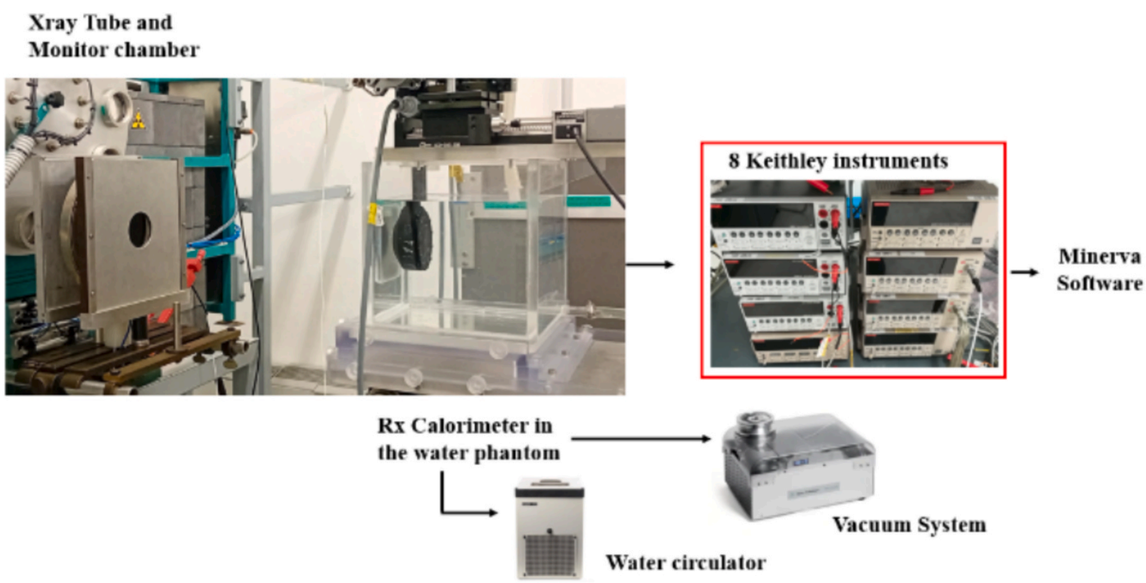

Fig. 7. Experimental irradiation setup.

Table 4
Fractional change in Resistance of the calorimeter's core thermistor from the mean value during X irradiation runs, analysis for different settings values.

CCRI 250	$f_C \Delta R/R$ (mΩ/Ω)	Mean value	Standard Deviation	Standard deviation of the mean
	Old setup	1.62E−05	9.22E−07	1.83E−07
	New setup	1.58E−05	6.83E−07	1.36E−07

enhancement significantly improves the metrological performance of the Italian primary standard for absorbed dose to water in medium-energy X-ray beams.

The final phase of the research, currently in progress, involves performing measurement tests across the full set of CCRI X-ray beam qualities, spanning the energy range from 100 kV to 250 kV. Further reports will focus on the calibration of various ionization chambers for the remaining X-ray qualities to provide a comprehensive overview and to support the presentation of the improved calorimeter performance at the upcoming K9 comparison.

The revised measurement setup reduces the standard deviation observed across repeated trials, thereby improving the Type A uncertainty. Although this enhancement contributes to greater precision, additional validation is necessary to determine whether the results exhibit improved reliability.

The main focus of the research activity at this stage is to improve the type A uncertainty on f_C that was predominant with respect to other uncertainty components (see Tables 1, 4 and 5). In the next steps, we will extend the study to further uncertainty components with the aim of minimising the overall uncertainty. A highly repeatable measurement system could provide a stable foundation for interlaboratory comparison K9 and supports the long-term reliability of the method.

While the present uncertainty evaluation has primarily addressed statistical components, we acknowledge that fitting procedures, particularly long-range linear fits, may also introduce systematic effects. The interaction between acquisition parameters and fitting behavior can influence the final uncertainty, especially in radiation calorimetry, where over-averaging or extended integration times may lead to Type B

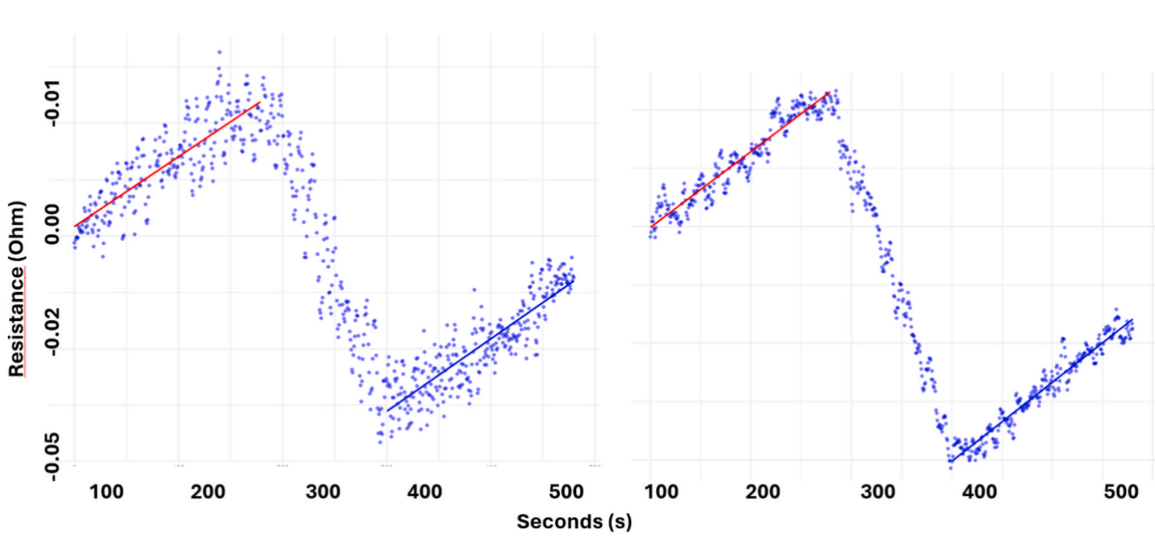

Fig. 8. Graphic calorimetric run comparison under irradiation. On the left side a run acquired with Delta mode off, Nplc 5 and Count 5, on the right side the run acquired with Delta mode on, Nplc 5, Count 20.

Table 5
Reduction in Type A uncertainty of f_C repeatability under irradiation, calculated as the standard deviation of the sample across runs for X-ray quality CCRI250.

Source of uncertainty	u_{iA}	u_{iB}
f_C, fractional change of the thermistor resistance	**0.0093**	0.0014
K_{qa}, quasi-adiabatic calibration coefficient	**0.0011**	0.0021
K_{vol}, core finite volume correction factor	0.0014	0.0010
K_{sc}, non-water equivalence of PMMA phantom's entrance window correction factor	0.0010	
Monitor chamber signal	0.0005	0.0021
Calorimeter positioning		0.0025
C_{wg} graphite to water absorbed dose conversion factor	0.0010	0.0087
K_{mass}, graphite mass correction factor	0.0010	0.0046
Quadratic sum	0.0096	0.0107
Combined relative standard uncertainty, D_w	0.0144	

contributions. These aspects will be further investigated in future developments to refine the uncertainty model and strengthen the metrological robustness of the approach.

The advancement of the Rx calorimeter's performance enables the National Institute of Ionizing Radiation Metrology to expand its measurement capabilities and offer new calibration services both nationally and internationally. The ongoing BIPM.RI(I)-K9 comparison plays a pivotal role in the harmonization of international standards and in strengthening confidence in absorbed dose measurements across metrology institutes worldwide.

CRediT authorship contribution statement

Susy Toma: Writing – original draft, Investigation, Data curation. **Massimo Pinto:** Conceptualization. **Fausto Arpino:** Supervision. **Domenico Capriglione:** Supervision, Methodology, Investigation, Conceptualization.

Declaration of competing interest

The authors declare that they have no known competing financial interests or personal relationships that could have appeared to influence the work reported in this paper.

Acknowledgments

The authors would like to thank the National Institute of Ionizing Radiation Metrology ENEA- INMRI in the ENEA Casaccia Research Center and at Industrial measurements laboratory, LAMI, of the Department of Electrical and Information Engineering DIEI of University of Cassino and Southern Lazio and all collaborators who contributed to the development of this work.

Data availability

The data that has been used is confidential.

References

[1] IAEA Code of Practice TRS 398, Absorbed Dose Determination in External Beam Radiotherapy, 2024.
[2] J. Renaud, H. Palmans, A. Sarfehnia, J. Seuntjens, Absorbed dose calorimetry, Phys. Med. Biol, Mar 2 (2020) 65(5):05TR02.
[3] https://www.irsn.fr/sites/default/files/documents/professionnels_sante/documentation/syllabus_chapitre_9.pdf.
[4] International Atomic Energy Agency, Accuracy Requirements and Uncertainties in Radiotherapy, IAEA Human Health Series No. 31, IAEA, Vienna, 2016.
[5] D.Y. Breitkreutz, M.D. Weil, M. Bazalova-Carter, External beam radiation therapy with kilovoltage x-rays, Phys. Med. 79 (2020) 103–112.
[6] Ludwig Büermann, Antonio Stefano Guerra, Maria Pimpinella, Massimo Pinto, Jacco de Pooter, Leon de Prez, Bartel Jansen, Marc Denoziere, Benjamin Rapp, First international comparison of primary absorbed dose to water standards in the medium-energy x-rays, EURAMET.RI(I)-S13 - Final report dated 2016-02-18.
[7] First international comparison of primary absorbed dose to water standards in the medium-energy X-ray range, Ludwig Büermann(a), Antonio Stefano Guerra(b), Maria Pimpinella(b), Massimo Pinto(b), Jacco de Pooter(c), Leon de Prez(c), Bartel Jansen(c), Marc Denoziere(d) and Benjamin Rapp(d).
[8] De Prez, De Pooter, Calorimetric determination of the absorbed dose to water for medium-energy x-rays with generating voltages from 70 to 280 kV, 2008.
[9] A. Krauss et al., Calorimetric determination of the absorbed dose to water for medium-energy x-rays with generating voltages from 70 to 280 kV, 2012.
[10] B. Rapp, N. Perichon, M. Denoziere, J. Daures, A. Ostrowsky, J.-M. Bordy, The LNE-LNHB water calorimeter for primary measurement of absorbed dose at low depth in water: application to medium-energy x-rays, Phys. Med. Biol. 58 (2013) 2769–2786.
[11] M. Pinto, M. Pimpinella, M. Quini, M. D'Arienzo, I. Astefanoaei, S. Loreti, A. S. Guerra, A graphite calorimeter for absolute measurements of absorbed dose to

water: application in medium-energy x-ray filtered beams, Phys. Med. Biol. 61 (2016) (2016) 1738–1764.
[12] Massimo Pinto and Maria Pimpinella, 16NRM03 RTNORM WP1 Report on ENEA-INMRI measurements of Farmer Chambers in water and in air (A1.2.2), activity 1.2.4 (cross calibrations), 1.2.6 (this report), and early contribution to Activity 1.2.8 (collective estimate of Transl. J. Magn. Japan, vol. 2, pp.
[13] Susy Toma, Massimo Pinto, Gianluca Cappadozzi, Carlo Di Ianni, Fausto Arpino, Domenico Capriglione, Reducing Type a Uncertainty of Quasi Adiabatic Calibration Factor in a Graphite Calorimeter for Radiation Dosimetry Measurements, IEEE Metroind&Iot 2025.
[14] S. Toma, M. Pinto, F. Arpino, D. Capriglione, Towards improving the metrological performance of a graphite calorimeter for radiation dosimetry measurements, Sens. Measur. (2024).
[15] S.R. Domen, P.J. Lamperti, A heat-loss-compensated calorimeter: theory, design, and performance, J. Res. Natl Bur. Stand. A 78 (1974) 595–610.
[16] Steve R. Domen, An Absorbed Dose Water Calorimeter: Theory, Design, and Performance", National Bureau of Standards, Washington, D.C. 20234, January 13, 1982.
[17] Ludwig Büermann, Antonio Stefano Guerra, Maria Pimpinella, Massimo Pinto, Jacco de Pooter, Leon de Prez, Bartel Jansen, Marc Denoziere and Benjamin Rapp, "First international comparison of primary absorbed dose to water standards in the medium-energy x-rays", EURAMET.RI(I)-S13 - Final report dated 2016-02-18.
[18] First international comparison of primary absorbed dose to water standards in the medium-energy X-ray range, Ludwig Büermann(a), Antonio Stefano Guerra(b), Maria Pimpinella(b), Massimo Pinto(b), Jacco de Pooter(c), Leon de Prez(c), Bartel Jansen(c), Marc Denoziere(d) and Benjamin Rapp(d).
[19] Massimo Pinto and Maria Pimpinella, 16NRM03 RTNORM WP1 Report on ENEA-INMRI measurements of Farmer Chambers in water and in air (A1.2.2), activity 1.2.4 (cross calibrations), 1.2.6 (this report), and early contribution to Activity 1.2.8 (collective estimate of Transl. J. Magn. Japan, vol. 2, pp. 740–741, August 1987 [Digests 9th Annual Conf. Magnetics Japan, p. 301, 1982].
[20] J. Williams, 775 Nanovolt Noise Measurement for a Low Noise Voltage Reference, Linear Technology Application Note AN124, July 2009.
[21] Keysight Technologies, Adjusting Nplc and Aperture to Make High-Speed Measurements, Application Note, 2020.
[22] Keithley Instruments, Model 2182a, user manual, LLC, Cleveland, Ohio, USA, 2022.
[23] Christensen et al., Using a small-core graphite calorimeter for dosimetry and scintillator quenching corrections in a therapeutic proton beam. Fonte: Phys. Med. Biol. 65(21).
[24] Tektronix, Configuring the Model 2460 for Delta Mode Measurements Using the 2182A Nanovoltmeter, Application Note, 2021.
[25] M.A. Khan, G. Dumstorff, C. Winkelmann, W. Lang, Investigations on noise level in AC- and DC-bridge circuits for sensor measurement systems, AMA Sci. Proc. IMSAS – Universität Bremen (2021).
[26] J. Renaud, S. Rossomme, A. Sarfehnia, J. Seuntjens, Development and application of a water calorimeter for the absolute dosimetry of short-range particle beams, Phys. Med. Biol. 61 (18) (2016) 6602–6620, https://doi.org/10.1088/0031-9155/61/18/6602.
[27] J. Witzani et al., A graphite absorbed-dose calorimeter in the quasi-isothermal mode of operation, 1984.